PLOS ONE

RESEARCH ARTICLE

Nitrate and Nitrite Variability at the Seafloor of an Oxygen Minimum Zone Revealed by a Novel Microfluidic In-Situ Chemical Sensor

Mustafa Yücel[1,2]*, Alexander D. Beaton[3], Marcus Dengler[1], Matthew C. Mowlem[3], Frank Sohl[4], Stefan Sommer[1]

1 GEOMAR Helmholtz Centre for Ocean Research, Kiel, Germany, **2** Middle East Technical University (METU), Institute of Marine Sciences, Erdemli, Mersin, Turkey, **3** National Oceanography Centre Southampton, Ocean Technology and Engineering Group, Southampton, United Kingdom, **4** DLR German Aerospace Center, Institute for Planetary Science, Berlin, Germany

* myucel@ims.metu.edu.tr

Citation: Yücel M, Beaton AD, Dengler M, Mowlem MC, Sohl F, Sommer S (2015) Nitrate and Nitrite Variability at the Seafloor of an Oxygen Minimum Zone Revealed by a Novel Microfluidic In-Situ Chemical Sensor. PLoS ONE 10(7): e0132785. doi:10.1371/journal.pone.0132785

Editor: Wei-Chun Chin, University of California, Merced, UNITED STATES

Received: March 13, 2015

Accepted: June 19, 2015

Published: July 10, 2015

Data Availability Statement: All relevant data are within the paper and its Supporting Information files.

Funding: This study was supported by the Helmholtz-Alliance ROBEX (Robotic Exploration of Extreme Environments - http://www.robex-allianz.de/en, funds to SS, FS) and the collaborative research center Climate-Biogeochemistry Interactions in the Tropical Ocean (SFB754 - www.sfb754.de, funds to SS, MD).

Competing Interests: The authors have declared that no competing interests exist.

Abstract

Microfluidics, or lab-on-a-chip (LOC) is a promising technology that allows the development of miniaturized chemical sensors. In contrast to the surging interest in biomedical sciences, the utilization of LOC sensors in aquatic sciences is still in infancy but a wider use of such sensors could mitigate the undersampling problem of ocean biogeochemical processes. Here we describe the first underwater test of a novel LOC sensor to obtain in situ calibrated time-series (up to 40 h) of nitrate+nitrite (ΣNO_x) and nitrite on the seafloor of the Mauritanian oxygen minimum zone, offshore Western Africa. Initial tests showed that the sensor successfully reproduced water column (160 m) nutrient profiles. Lander deployments at 50, 100 and 170 m depth indicated that the biogeochemical variability was high over the Mauritanian shelf: The 50 m site had the lowest ΣNO_x concentration, with 15.2 to 23.4 μM (median=18.3 μM); while at the 100 site ΣNO_x varied between 21.0 and 30.1 μM over 40 hours (median = 25.1μM). The 170 m site had the highest median ΣNO_x level (25.8 μM) with less variability (22.8 to 27.7 μM). At the 50 m site, nitrite concentration decreased five-fold from 1 to 0.2 μM in just 30 hours accompanied by decreasing oxygen and increasing nitrate concentrations. Taken together with the time series of oxygen, temperature, pressure and current velocities, we propose that the episodic intrusion of deeper waters via cross-shelf transport leads to intrusion of nitrate-rich, but oxygen-poor waters to shallower locations, with consequences for benthic nitrogen cycling. This first validation of an LOC sensor at elevated water depths revealed that when deployed for longer periods and as a part of a sensor network, LOC technology has the potential to contribute to the understanding of the benthic biogeochemical dynamics.

Introduction

In situ, high frequency observations are crucial to uncover the temporal and spatial complexity in the aquatic environments [1]. Considerable progress has been made with the increasing use of in situ sensors on a variety of platforms; however these devices mostly address physical parameters such as temperature, light or pressure [2, 3]. On the other hand, with the notable exception of oxygen [4,5], pH [6] and nitrate at low (μM) resolution (see below), routine calibrated and accurate measurements of chemical parameters still depend on spatially and temporally limited sampling schemes and subsequent analyses onboard research vessels or in shore-based laboratories. Hence, the biogeochemical variability of oceanic habitats is so far largely unknown but is ultimately important to understand the productivity, elemental cycles and ocean response to a changing global climate.

As a limiting nutrient of biological productivity, nitrate (NO_3^-) and nitrite (NO_2^-) are among those parameters for which several sensor technologies already exist, such as a UV-spectrophotometry based system reported by Johnson et al. [7] (also see [8, 9]), and the colorimetric system by Le Bris et al. [10] (for reviews see [11–13]). Some nitrate sensors have become commercially available (such as Satlantic ISUS, Systea WIZ), and recent applications of these sensors uncovered the high temporal variability in NO_3^- in the open ocean [8]. The temporal variability can be even higher in estuaries, where current can be fast and freshwater inputs are significant [14]. Despite these improvements, the capacity of many nutrient sensors to perform long term, stable measurements at elevated water depths may be limited due to shallow depth range, large size, large power consumption and/or high detection limits.

The bottom waters of oceanic oxygen minimum zones (OMZ) are one of those environments for which there is almost no information on the short-term temporal nutrient variations. Here, the availability of NO_3^-/NO_2^- drives the anaerobic degradation of organic matter in the water column and the sediment surface [15]. Moreover, these electron acceptors are involved in the anaerobic oxidation of NH_4^+, which is released in high amounts from the seafloor under anoxic conditions [16, 17]. In organic-rich sediments NO_3^-/NO_2^- can be further involved in the oxidation of sulfides [18]. Besides consumption and production, physical transport processes such as currents, submesoscale eddies or passage of internal waves can also drive the variability of these nutrients over continental shelves below OMZs [19].

To accurately constrain the variability of NO_3^-/NO_2^- at the seafloor of an OMZ, we need pressure-insensitive, robust sensors with the capability of in situ calibration. The in situ calibration is particularly important for an application at a fixed point at the seafloor, where there is potential for variability over short time scales. In this regard, microfluidics, or 'lab-on-a-chip' (LOC) is a promising technology that meets several demands needed for autonomous measurements at elevated depth such as low weight, low energy demand, and low volume consumption of reagents and samples [20, 21] and ease of integration into underwater platforms. Having been mostly developed for medical and pharmaceutical research [22], LOC technology is now being transferred to aquatic environmental research as well [23–27]. Newly developed LOC devices can measure not only NO_3^- and NO_2^-, [23, 26, 27] but also PO_4^{3-} [28] and dissolved Fe and Mn [29]. Among these devices, the NO_3^- / NO_2^- LOC system is approaching maturity for time-series applications but, prior to the work reported here, its suitability for the in situ deployment at elevated depth has not been demonstrated.

Using a new generation LOC sensor that was capable of in situ calibration, we report the first in situ time series (up to 40 h) of NO_3^- + NO_2^- (ΣNO_x) and NO_2^- at the seafloor (max. 170 m depth) in an upwelling region offshore Western Africa. We combine these data with time series of oxygen, temperature and bottom currents to demonstrate that the LOC

technology provides a previously unavailable window into the variability of nutrient concentrations in the bottom waters of a low-oxygen coastal ocean.

Methods

Study Area

The study site was near 18°N in the Mauritanian upwelling region which is part of the Canary eastern boundary upwelling system that roughly extends between 43°N to 10°N [30, 31]. Fieldwork permit was obtained from Mauritanian Ministry of Fisheries and Maritime Economy (*Ministère des Pêches et de l'Economie Maritime*, Permit No: 296, dated May 14, 2014). Coastal upwelling near 18°N off Mauritania exhibits a pronounced seasonality where winds favorable to upwelling prevail primarily from December to April. Due to the weak mean circulation in the eastern tropical Atlantic, an oxygen minimum zone is situated below the surface layers. While the core of the main OMZ is found at about 400 m depth, a secondary oxygen minimum is situated below the surface mixed layer and above 200 m depth [32]. The ventilation of the waters above the continental margin occurs primarily through the Mauritania Current [33] in the near-surface layers and the Poleward Undercurrent below [34]. Both currents transport relatively oxygen-rich South Atlantic Central Water, which is supplied by the eastward flowing North Equatorial Countercurrent and North Equatorial Undercurrent, northward into the upwelling region.

A physical-biogeochemical measurement program was performed during the R/V Meteor cruise M107 from May 28 to July 3, 2014 during the termination period of the upwelling season as a part of a collaborative research center Climate-Biogeochemistry Interactions in the Tropical Ocean (SFB754) and the Helmholtz-Alliance ROBEX (Robotic Exploration of Extreme Environments). The observational program included benthic lander deployments, conductivity-temperature-depth-oxygen (CTD/O_2) profiling paired with water sampling and mooring deployments measuring currents and hydrography along a transect at 18°N.

Lander deployments at the Bottom Boundary Layer

A GEOMAR benthic lander (thereafter as the Lander) was used as a platform to make autonomous in situ measurements [35]. The Lander was deployed on the sea floor at depths of 50, 100 and 170 m (Table 1). These depths were chosen as bottom water oxygen time series displayed high variability during a previous cruise [36] (R/V MS Merian leg 17/4) and benthic nitrogen turnover rates were high due to hypoxia [17]. At all locations, the LOC sensor (Ocean Technology and Engineering Group, National Oceanography Centre Southampton) was attached to the lander and at the 50 and 100 m sites this LOC system was complemented with a CTD probe (RBR, Ottawa, Canada) and an O_2 optode (Aandrea, Bergen, Norway). For the deployment at the 50 m site an additional LOC sensor measuring NO_2^- was added. Prior to the Lander

Table 1. Details of underwater operations during R/VMeteor cruise M107 where autonomous measurements were performed.

Depth (m)	Operation	RV Meteor Station	Longitude (N)	Latitude (W)	Measured Parameters	Measurements Start (2014, UTC)	Measurements End (2014,UTC)
50	Lander 3	M107-687	18°17.0'	16°19.0'	NO_3^-+ NO_2^-, NO_2^-, O_2, CTD	June 25, 15:00	June 26, 23:00
100	Lander 2	M107-633	18°14.7'	16°27.0'	NO_3^-+ NO_2^-, O_2, CTD	June 21, 15:00	June 23, 07:00
170	Lander 1	M107-572	18°14.2'	16°31.0'	NO_3^-+NO_2^-	June 13, 16:00	June 14, 14:00
170	CTD #16	M107-559	18°14.0'	16°31.0'	NO_3^-+NO_2^-	June 12, 15:00	June 12, 17:10
50	POZ Lander	M107-505	18°16.0'	16°19.0'	Current velocity	June 8, 18:00	June 27, 07:00
50	BIGOII-4 Lander	M107-665	18°17.1'	16°19.0'	NO_2^-, syringe samples		

doi:10.1371/journal.pone.0132785.t001

deployments, the LOC sensor was tested in situ on the CTD rosette to compare the sensor results to concentration measurements from water samples analyzed on-board using an autoanalyzer (Quattro, Seal Analytical, UK).

Application of the Lab-on-Chip Nitrate/Nitrite Sensor

The LOC ΣNO_x sensor was previously described in detail by Beaton et al. [23, 26]. That paper as well as Ogilvie et al. [37] and Floquet et al. [38] described various aspects of the lab-on-a-chip approach for nutrients. In short, the chip used in the sensor was made up of PMMA and harbored precision-milled microchannels (< 300 μm), mixers and optical components such as LEDs (525 nm) and photodiodes. An integrated syringe pump, valves and electronics complemented the chip and are encased in mineral oil-filled housing (PVC, 12 cm diameter, 30 cm height) with an internally fitted pressure-compensating bladder. The system ran autonomously storing the data in a memory card and was powered by an external battery. The unit weighed 1.1 kg in water without and 1.5 kg with an internal battery.

The sensor uses attached standards and blank for regular in situ calibrations along with sample (0.45 μm filtered) measurements, using the colorimetric Griess assay for NO_2^- detection [39]. The addition of an off-chip Cu-activated Cd column enabled NO_3^-+NO_2^- (ΣNO_x) detection through the reduction of NO_3^- to NO_2^- and subsequent on-chip analysis with a detection limit of 20 nM, an accuracy of 0.6% and a precision of 7 nm at low concentrations or 0.5% at high concentrations [23]. The deployment involved externally attached gas impermeable Flexboy bags (150 mL, Sartorius, UK) that contained two standard solutions (for either ΣNO_x or NO_2^-, as needed), Griess reagent, artificial seawater blank and imidazole buffer. The preparation of the standards and reagents followed previous protocols [40, 23, and 26]. Waste was collected in a 500 mL Flexboy bag. For example, for a deployment to measure ΣNO_x, the sensor started to perform two sets of calibrations (artificial seawater blank and 11.3 and 33.9 μM standards for NO_3^-) followed by a repeating sequence involving the measurement of blank, sample, standard solution and sample again. Each of these steps included 6 flushing cycles to avoid any carryover. The final flush cycle was followed by a 100-second waiting stage that enabled color development and the photometric measurement at 525 nm. A set of flushes and the waiting stage altogether took about 7 minutes. The sensor recorded optical absorbance every 1 second and the average of the last 3 reading of the waiting stage was used for calculations. Raw data were processed in R 3.0.2 [41]. With this scheme, we obtained one blank-corrected sample measurement every 14 minutes and one standard solution measurement every 28 minutes during deployment. For NO_2^- measurements, the off-chip Cd column was replaced with a short tube. The sensor operated the same as ΣNO_x sensor, with the only exception that the standard solutions of 0.5 and 2 μM NO_2^- were used.

Results and Discussion

First tests of the LOC analyzer at elevated depth

Two mid-depth O_2 minima, sharp nitracline (increasing nitrate concentration over a relatively small depth range in the water column) and a subsurface NO_2^- peak were persistent features in different CTD casts at the Mauritanian Shelf (one example shown in Fig 1A). Before the Lander deployments, we assessed the quality of the LOC sensor to reproduce vertical nutrient gradients by comparing it to concentrations obtained from water samples. It was therefore attached to the CTD frame during a profile to a depth of 160 m (CTD #16, S1 Fig). The sensor started to perform two sets of calibrations while the CTD was being lowered to 160 m. During the upcast, the rosette was stopped for 14 minutes at 7 different depths to allow for the in situ analysis of the blank (or a standard) and a sample. In the final minute of this period, a Niskin bottle

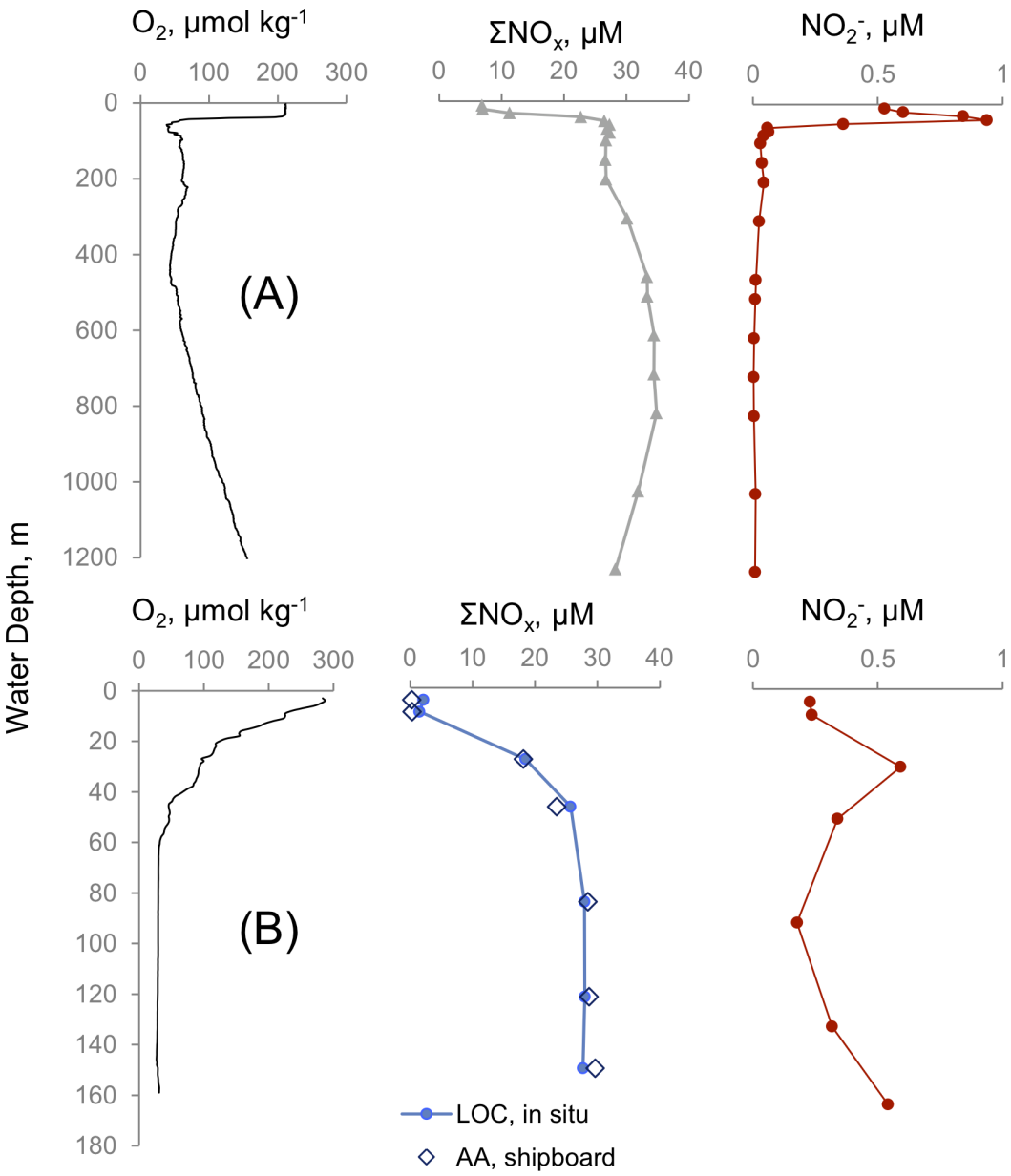

Fig 1. Water column chemistry in two stations in the Mauritanian OMZ (A) Water column profile of oxygen, NO_3^-+ NO_2^- (ΣNO_x) and NO_2^- during a CTD cast (#15) at 1200 m depth. Both casts were conducted on June 12, 2014 at 16°48.32' W and 18°09.00' N. (B) Profiles from CTD cast #16 at a depth of 160 m where a LOC sensor was also attached to the CTD frame. "AA" stands for autoanalyer. These profiles were obtained on June 12, 2014 at 18°14.0' W and 16° 31.0' N.

doi:10.1371/journal.pone.0132785.g001

sample was taken. Overall, the ΣNO_x distribution obtained from the LOC agreed well with the distribution of ΣNO_x obtained from shipboard autoanalyzer (AA) water samples (Fig 1B). All profiles showed that ΣNO_x was depleted at the surface with a nitracline located at about 20–40 m depth, below which ΣNO_x increased to about 30 µM. The location of the nitracline coincided with a NO_2^- concentration peak of 0.6 µM at 30 m, which was also the upper boundary of the O_2 minimum (29 µM after 60 m) extending down to 160 m.

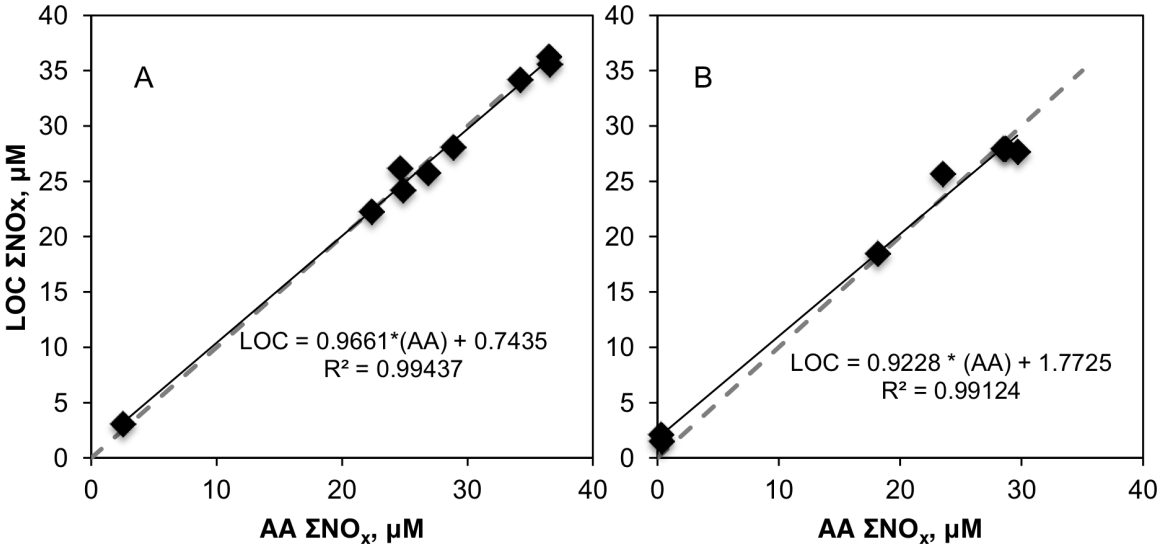

Fig 2. Comparison of autoanalyzer (AA) and LOC measurements (A) Autoanalyzer and LOC ΣNO_x measurements on samples obtained from hydrocast CTD#2, from 1000 m. Here, LOC was operated on a shipboard laboratory bench. (B) Autoanalyzer and in situ LOC ΣNO_x measurements on samples obtained from hydrocast CTD#16, from 170 m.

doi:10.1371/journal.pone.0132785.g002

Analytical Uncertainty Assessment

In addition to the submerged LOC tests during hydrocasts, we have performed additional comparisons (LOC measurement also shipboard) on bottle samples from another hydrocast at 1000 m (CTD#2). The combined scatter plots showing autoanalyzer (AA) and LOC measurements during CTD#2 and 16 (Fig 2) indicate that the results from the two approaches are highly correlated ($R^2 > 0.99$). The differences at high (>5 μM) concentrations were comparable to the estimated uncertainties of the two approaches, which were calculated from two times the standard deviations of successive calibrations (on board for autoanalyzer and in situ for LOC). This analysis yielded a value of ±0.1 μM for the autoanalyzer and ±0.4–1 μM for the LOC analyzer (summarized in Table 2). Considering these inherent analytical uncertainties with the differences in sample handling by different operators, we can assert that the LOC nutrient sensor was capable of delivering in situ measurements at elevated depth with an analytical performance only slightly less precise than the established techniques.

Table 2. Summary of the analytical performance derived from in situ measurements of standard solutions (for LOC) and on board measurements (Autoanalyzer).

Series	Calibration solution, μM	Number of measurements	% Standard deviation from mean *	Estimated uncertainty, μM **
170 m ΣNO_x	33.9	46	0.6	0.40
100 m ΣNO_x	11.3	85	4.3	0.98
50m ΣNO_x	11.3	63	3.4	0.76
50m NO_2^-	2.0	63	1.6	0.08
Autoanalyzer	5.8	10	0.8	0.10

* Average value of the moving (5) standard deviations

** Calculated as the average of concentrations corresponding to 2 times the moving (5) standard deviations. These uncertainties are also shown on Figs 3 and 4.

doi:10.1371/journal.pone.0132785.t002

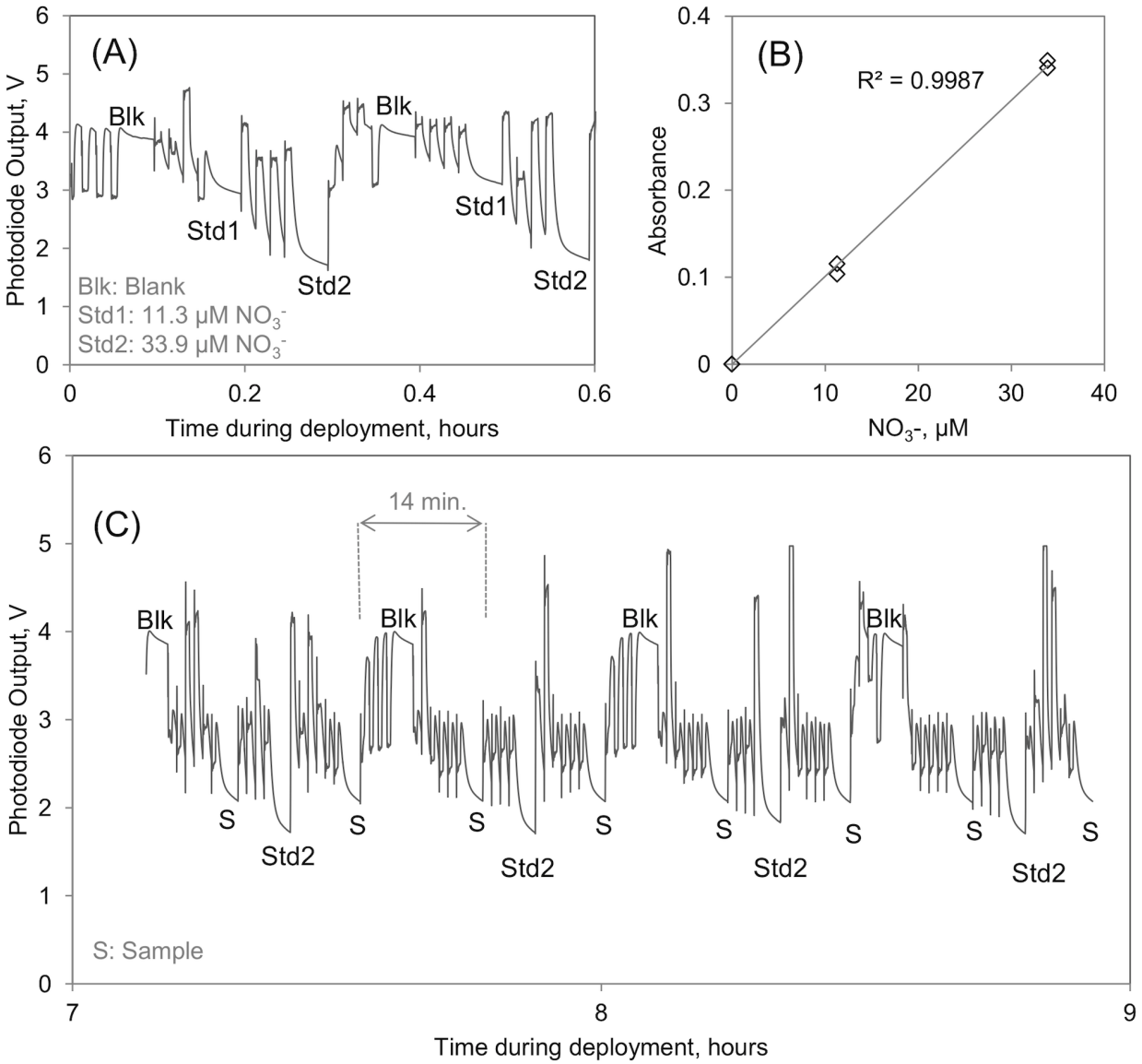

Fig 3. An example of the raw output of the lab-on-chip nitrate sensor. (A) Photodiode output showing the two sets of calibration performed in situ in the beginning of the series at 170 m depth. After the measurement of a blank (Blk), two standards solutions of NO_3^- (Std1 and Std2) were measured and the calibration plot in (B) was obtained. Panel (C) shows an excerpt of the photodiode output during the same time series at 170 m depth, 7–9 hours after the first measurement. Blank solutions and the 33.9 µM standard solution were regularly measured in between sample (S) measurements, The fluctuating voltages were recorded during the flushing of the microfluidic chip and do not affect the measurements themselves.

doi:10.1371/journal.pone.0132785.g003

In addition to the water sample comparison to validate sensor performance, it was also verified that the sensor performed reproducible in situ calibrations throughout all deployments, essential to obtain reliable time series data. An excerpt of raw photodiode readings featuring in situ blank, standard and sample measurements during the deployment at 170 m is shown in Fig 3. During all deployments no significant drift in the in situ calibrations was observed, however a random variability was present between successive calibrations from which sensor uncertainties were estimated (Table 2). The one blank-corrected sample per 14-minute measurement frequency used in this work should be considered as a minimum because we have aimed to fully utilize the in situ calibration feature and we had to use relatively high number of

6 flushing cycles due to high NO_3^- concentrations. Although we have not investigated a full optimization, we think that the frequency can increase to 1 measurement per 10 minutes with less frequent blank/standard analyses. Using a smaller number of flushing cycles can further increase the sample analysis frequency for low concentration samples (<5 μM). Use of newly emerging microfluidic architectures such as multiplexed stop flow [42] can enable multiple simultaneous measurements on the same chip, increasing the frequency to one sample per minute or more.

Nitrate and nitrite dynamics in the bottom boundary layer

The CTD casts only provided a snapshot of a dynamic system while the time series for ΣNO_x from the bottom waters at 50, 100 and 170 m (Fig 4) revealed high variability. The 50 m site had the lowest ΣNO_x concentrations (15.2 to 23.4 μM) while the 100 m site had a larger ΣNO_x range (21 to 30.1 μM) recorded in 40 hours. Over a 20-hour period, the 170 m site had ΣNO_x levels ranging from 22.8 to 27.7 μM, with 5–8 hours of very stable levels interrupted by more variable values. The median values of the time series measurements increased with depth, consistent with the trend suggested by the water column profiles. While the long-term (hours) variability was remarkable (discussed in detail in the next section), short-term variability on time scales less than hour was also high in certain periods. To compare the inherent sensor precision with natural variability, we have also plotted a 'moving uncertainty', calculated from two times the moving (n = 5) standard deviations of the successive in situ measurements of a standard solution (Fig 4 and Table 2). This comparison showed that most of the short-term variation less than a micromolar could be attributed to sensor response. However at certain periods there were marked deviations from the expected uncertainty, such as those in the 170 m time series (Fig 4C). The most likely physical explanation for the short-term ΣNO_x variability is the propagation of bores and non-linear internal wave trains, observed at the upper continental slope and the shelf off Mauritania at 18°N [19]. They are generated by interaction of barotropic and low-mode baroclinic tides with topography [43] and propagate onshore. Individual non-linear internal waves within the bores exhibited periods of 10 to 15 minutes and associated vertical velocities exceeded 0.15 m s^{-1} while on the continental slope they were particularly pronounced between 75 and 200m depth [19]. During their passage, they vertically displace water over a depth range of more than 70m. Thus we hypothesize that the short-term variability was due to the downward displacement of water having lower ΣNO_x concentrations from above. Non-linear internal waves have been observed on continental slopes in many continental slopes in the world ocean [44]. We suggest that they cause elevated high-frequency variability of near-bottom ΣNO_x concentrations and other solutes having vertical concentration gradients in the lower 50m to 100m of the water column, which may affect biogeochemical processes in the sediments and within the bottom boundary layer.

At 50m, a location near the subsurface NO_2^- peak (Fig 1), we deployed a second LOC system that measured NO_2^- only in addition to the LOC measuring ΣNO_x. The real-time clocks of the two sensors were synchronized, which enabled measurement of NO_2^- simultaneously with NO_3^- via subtracting NO_2^- from ΣNO_x. In the series, shown in Fig 5, NO_2^- decreased from 1 μM to about 0.2 μM within 30 hours. Nitrate increased through the series with decreasing NO_2^-, suggesting a different water mass moved in, possibly originating from deeper waters where NO_3^- is high and NO_2^- is low. Remarkably, a similar magnitude of variability in the NO_3^- NO_2^- relationship was documented by measurements of bottom water samples sequentially taken via another benthic lander deployment (BIGOII-4, see Table 1) at the same position measuring benthic fluxes. This was deployed for two days prior to the Lander deployment and stopped sampling about 13 hours before the LOC sensors started measuring at the same depth.

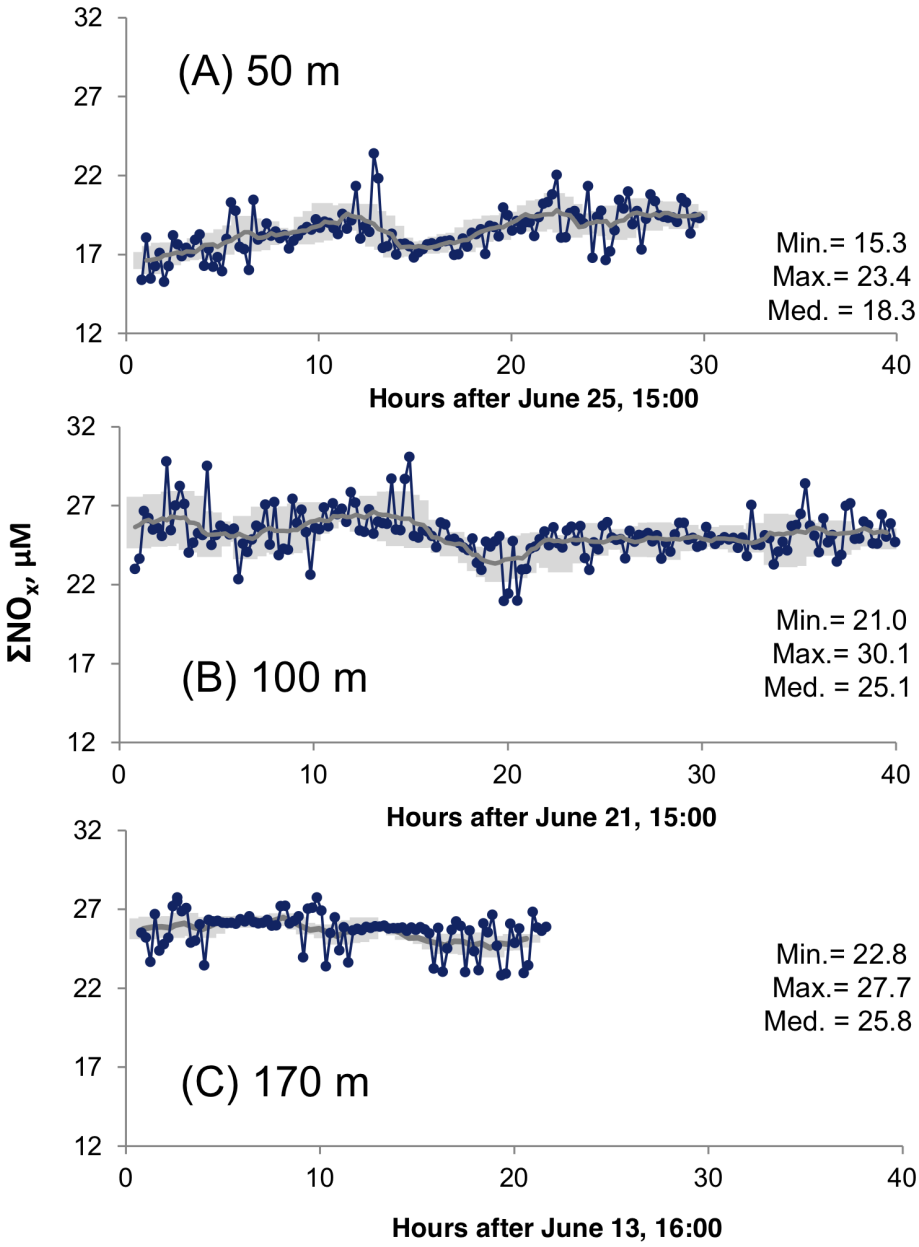

Fig 4. Time series measurements of NO3-+ NO2- (ΣNO_x) in bottom waters. The time axis indicates time starting from the first sensor measurement in each respective deployment (see Table 1 for dates). The gray line in each series denotes a 12-point moving average. Also plotted as gray shading is 'moving uncertainity' corresponding to concentrations calculated from two times the moving (n = 5) standard deviations of the successive in situ measurements of a standard solution (Table 2). Any point outside the gray area very likely reflects natural variability.

doi:10.1371/journal.pone.0132785.g004

When LOC measurements are appended to the results of the discrete bottom water measurements (Fig 5, inset), a more complete picture emerges where the starting NO_2^- poor, NO_3^- rich waters were replaced by waters higher in NO_3^- and lower in NO_2^- through the middle of series. At the end of this period, the bottom water chemistry returns to the starting composition, suggesting a ~3 day cycle.

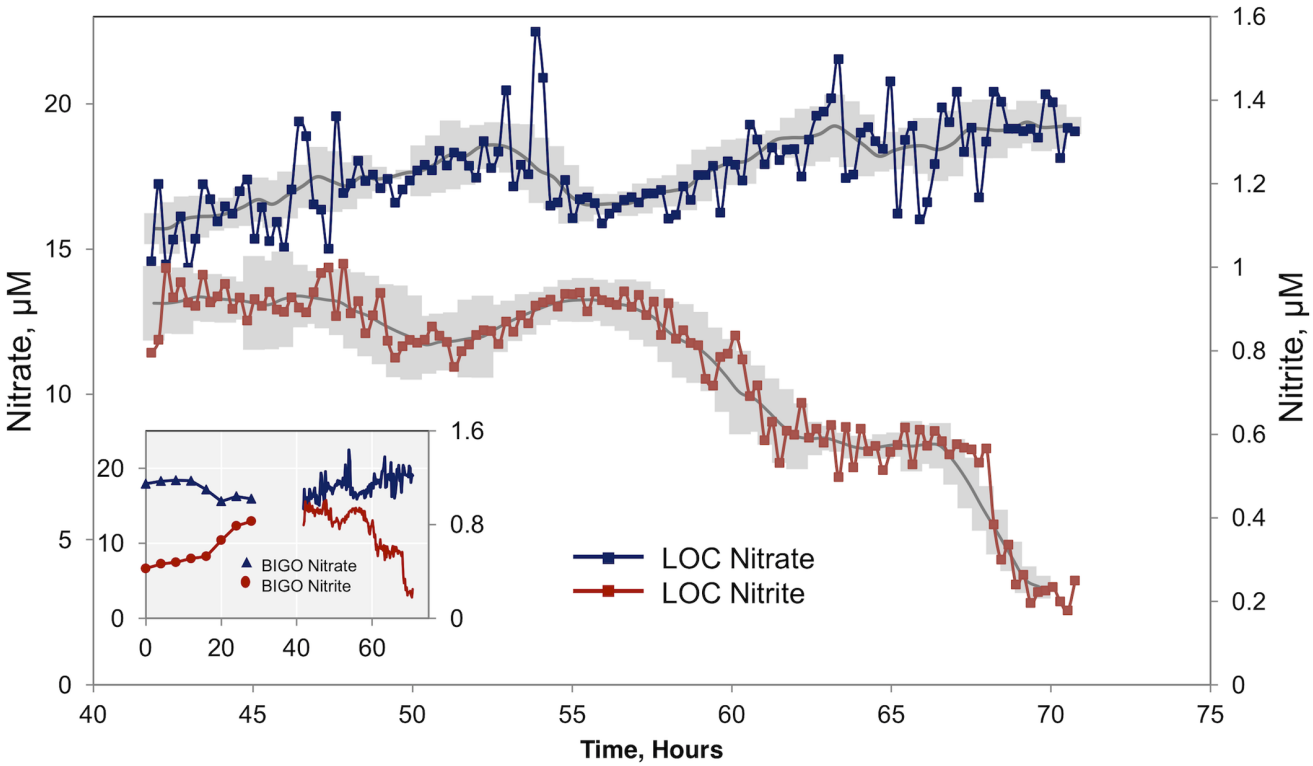

Fig 5. Simultaneous measurements of NO_3^- and NO_2^- at 50 m depth. Gray lines indicate 12-point moving averages. Also plotted as gray shading are 'moving uncertainities' calculated from two times the moving (n = 5) standard deviations of the successive in situ measurements of a standard calibration solution. The data from bottom water samples from a previous lander deployment (BIGOII-4) at this depth are also given in the inset. The time zero is set at the beginning of the BIGOII-4 deployment. When the time series from the lab-on-chip sensor are appended to the BIGOII-4 data (inset), a 3-day cycle emerges where the original NO_2^- poor, NO_3^- rich bottom water is replaced by water of higher NO_2^- and lower NO_3^-. The water chemistry returns to original situation at the end of the 72-hour series.

doi:10.1371/journal.pone.0132785.g005

Drivers of the long-term (hours) benthic biogeochemical variability

In order to account for the observed variability of nutrients over several hours, we also recorded physical parameters and oxygen at the 50 and 100m sites (Fig 6). In both sites, the tides did not explain any of the nutrient variability. Cross correlation matrices of the series (S2 Fig) revealed that the 50 m site had more correlated pairs than the 100 m site. Considering this difference, and the fact that our dataset is more complete for the 50 m site, we focus our discussion on the 50 m site. At the 50 m series, the NO_2^-, which correlated inversely with NO_3^- (Spearman Rank Correlation, $r = -0.59$, $p<0.01$), also had a significant inverse correlation with temperature (T) ($r = -0.52$, $p<0.01$) and positive correlation with O_2 ($r = 0.58$, $p<0.01$). Nitrate had weaker, but still significant correlations (in opposite sign to that of NO_2^-) with these parameters. Taken together, these findings suggest that during the course of the 50m time series NO_3^- rich NO_2^- -poor cooler waters replaced the original warmer, O_2-rich, NO_2^- rich waters. Therefore the overall trend was towards increasing temperatures, decreasing NO_2^- and O_2 while increasing NO_3^- (Fig 4 and Fig 6a).

What drives these non-tidal variations in the chemical and physical parameters? To attempt an explanation we examined the velocity profiles from an acoustic Doppler current profiler (ADCP) that was deployed on the sea floor at the depth of 50 m, close to the Lander deployment site (Table 1). Over a 15-day period, the alongshore and across-shore currents fluctuated

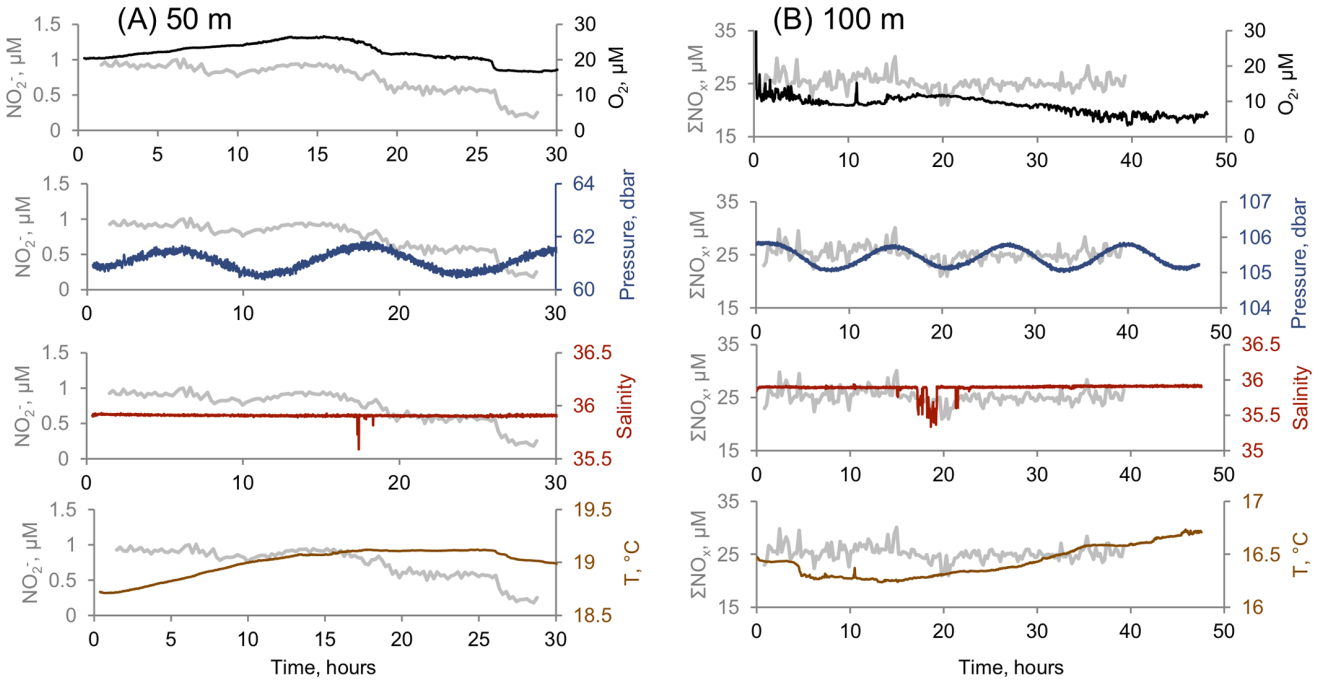

Fig 6. Time-Series of other parameters obtained during the lander deployments. (A) Time series of O_2, pressure, salinity and temperature (black) plotted with NO_2^- series (gray) in the 50 m site. (B) Time series of O_2, pressure, salinity and temperature (black) plotted with ΣNO_x series (gray) in the 100 m site.

doi:10.1371/journal.pone.0132785.g006

significantly reaching velocities of 0.4 m s^{-1} (Fig 7). Close to the sea floor at 45–50 m depths, a notable northward flow existed with intermittent onshore and offshore flow. Focusing on the period of chemical time series at 50 m (June 23–27 2014, Fig 7); we found that the high- NO_2^- low- NO_3^- period coincided with the maximum northward alongshore flow in much of the water column and elevated offshore flow in the near bottom layer. When the alongshore flow decreased on June 26, an onshore flow in the near bottom layer became pronounced attaining velocities up to 0.1 m s^{-1}. The change in the current direction is coincident with the steep decrease in NO_2^-, and indicates deep-water movement towards the shore.

The correlation between near-bottom onshore flow variability and alongshore flow variability in the water column can be interpreted in terms of bottom-boundary layer Ekman dynamics. Due to bottom friction and the Coriolis force, a northward alongshore flow above the bottom boundary layer will generate an offshore flow component in the bottom boundary layer, which is in agreement with velocity time series (Fig 7). Thus, during the period of elevated northward flow on the shelf, the intrusion of deeper waters was blocked and water masses from the shallower shelf regions that were low in NO_3^- and high in NO_2^- were advected offshore. When the northward current ceased, deeper waters started to move on shore, which resulted in higher NO_3^-, lower NO_2^- and lower O_2 concentrations (Fig 6). While the northward flow on the shelf can generally be attributed to the Mauritanian current during this period [32], the elevated northward velocities between June 22 and June 26 represent an intermittent feature that is probably due to local wind forcing. One biogeochemical implication is that these fluctuating currents may lead to periodic pumping of deep waters at the 50 m site. At this shallow site this might be an important mechanism for nutrient transport to support primary production as well as for the supply of electron acceptors to drive denitrification and the

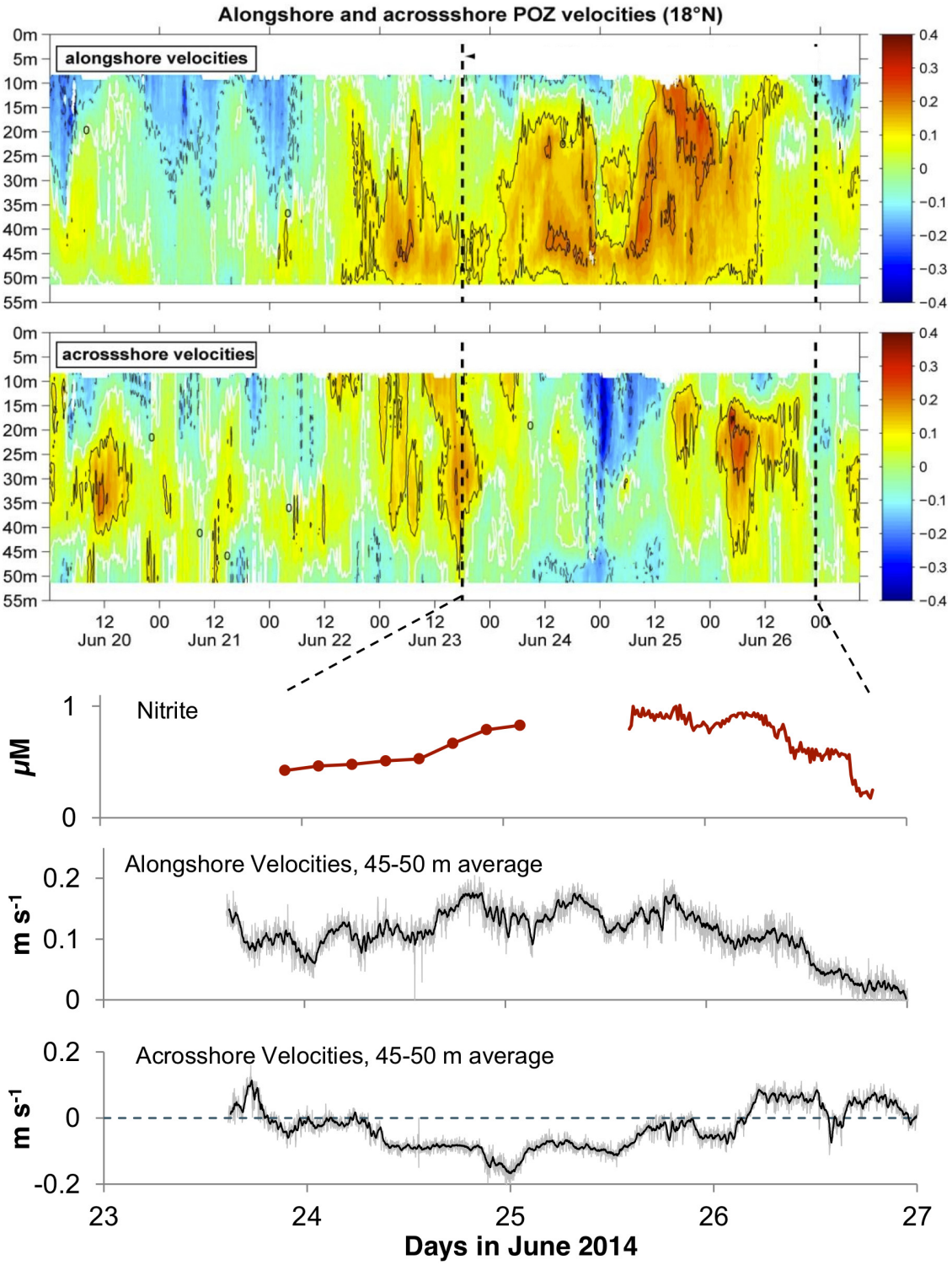

Fig 7. Alongshore and across shore velocities (m s^{-1}) at the 50 m site. The velocities were measured with an upward-looking ADCP on a lander at 50m on the 18° N transect. Positive alongshore velocities values stand for northward flow while positive across shore velocities represent flow towards the shore. The NO_2^- (μM) series shown in Fig 4 are also added to indicate that the high- NO_2^- periods were associated with strong positive alongshore velocities and negative across shore velocities.

doi:10.1371/journal.pone.0132785.g007

subsequent nitrogen redox process in the upper sediments. While the hydrodynamically-driven variability in NO_3^- concentrations is pronounced in the seafloor of the Mauritanian Upwelling, the variability is even more dramatic for NO_2^- when relative changes are considered (Fig 5). At the 50 m site, the bottom water NO_2^- concentration decreased fivefold, from 1 μM to 0.2 μM in just 30 hours. Porewater NO_2^- concentrations in the surface sediments at this site were in the order of several hundred nanomolars (ref. [17] and unpubl. data from M107). Hence, the dramatic change in the bottom water NO_2^- concentration can influence the direction and magnitude of the benthic NO_2^- fluxes. Future longer-term deployments with a network of nutrient sensors can answer questions such as whether or not this dramatic variability in NO_2^- exists at other sites and how this variability should be accounted for in determining the benthic biogeochemical feedback in this productive coastal ocean.

Conclusions and Future Perspectives

We have successfully deployed a new prototype microfluidic lab-on-chip (LOC) NO_3^-/ NO_2^- sensor in the bottom waters of a productive coastal ocean. To our knowledge this is the first report of time series from a LOC NO_3^-/ NO_2^- sensor in a deep underwater setting. We found that the analytical performance of the sensor at elevated depth was comparable to a conventional autoanalyzer. Coupled to time series measurements of oxygen and currents, the LOC measurements recorded large variations in nutrients, probably linked to cross-shelf water transport occurring in relation to the dynamics of the alongshore flow on the Mauritanian shelf. Relative variability of NO_2^- in the bottom waters was larger and this could affect the magnitude and direction of benthic biogeochemical fluxes in this low-oxygen coastal ocean.

Although we have not tested the LOC sensor in situ at depths beyond 170 m, our results show that the microfluidic sensor approach is not compromised by elevated pressures and therefore has a high potential for deep-water applications. New developments in sensor technology (such as miniaturization and new microfluidic architectures) are expected to decrease the size of these devices, allow the introduction of new chemical parameters, increase data acquisition frequency and enhance the applicability of the sensor towards Lagrangian (moving) platforms. These developments will not only be beneficial to Earth observation but also to space and planetary exploration—indeed this motivation was the starting point of our sensor testing work under the framework of Helmholtz Alliance ROBEX (Robotic Exploration of Extreme Environments) [45]. Particularly, having robust sensors at high technological maturity for underwater applications could contribute to future missions to active icy moons such as the Jovian moon Europa and Enceladus in the Saturnian system [46]. As the potential habitability of these moons is receiving increasing attention; the detection of biosignatures, dissolved nutrients or energy-yielding chemicals in the subsurface oceans [47] of these icy satellites would considerably benefit from in-situ analysis. In order to support this vision, and more specifically to increase the technological readiness of the new sensors, we need to continue to bring new generation chemical sensors to extreme environments such as deep sea, assess their capabilities and limitations and eventually implement sensor networks that will pave the way for more extensive testing and the much-needed highly resolved in situ biogeochemical datasets.

Supporting Information

S1 Fig. The LOC sensor as attached to the CTD rosette and the benthic lander.
(TIFF)

S2 Fig. Cross correlation matrices for the multi-parameter datasets obtained from 50 and 100m. Units are μM for NO_2^-, NO_3^- and O_2; dbars for pressure and °C for temperature. Stars indicate significant correlation ($p<0.01$) between the pair.
(TIFF)

S1 File. All data from the LOC sensors and autoanalyzer measurements on bottle samples.
(ZIP)

S2 File. All data from the POZ landers on the current measurements in the bottom waters.
(ZIP)

Acknowledgments

We thank the Captain and crew of RV Meteor cruise M107 for a very productive research cruise in the Eastern Atlantic. In situ sensor deployments would not have been possible without the excellent support from Sonja Kriwanek, Matthias Türk and Asmus Petersen. We thank Andy Dale, Bettina Domeyer and Anke Bleyer for the autoanalyzer nutrient measurements. Lastly, MY would like to thank the members of the NOC OTEG group for their hospitality and support during his research visits to Southampton.

Author Contributions

Conceived and designed the experiments: MY ADB MD MCM FS SS. Performed the experiments: MY MD SS. Analyzed the data: MY ADB MD SS. Contributed reagents/materials/analysis tools: ADB MD MCM FS. Wrote the paper: MY ADB MD MCM FS SS.

References

1. Mann KH, Lazier JRN. Dynamics of Marine Ecosystems: Biological-Physical Interactions in the oceans. Blackwell Publishing, 3rd Edition, Carlton, Australia, 2006.
2. Bellingham JG, Rajan K. Robotics in Remote and Hostile Environments. Science 2007; 318: 1098–1102 PMID: 18006738
3. Dickey TD, Itsweire EC, Moline MA, Perry MJ. Introduction to the Limnology and Oceanography Special Issue on Autonomous and Lagrangian Platforms and Sensors (ALPS). Limnol. Oceanogr. 2008; 53: 2057–2061.
4. Tengberg A, Hovdenes J, Andersson JH, Brocandel O, Diaz R, Hebert D, et al. Evaluation of a lifetime-based optode to measure oxygen in aquatic systems. Limnology and Oceanography-Methods 2006; 4: 7–17.
5. Takeshita Y, Martz TR, Johnson KS, Plant JN, Gilbert D, Riser SC,et al. A climatology-based quality control procedure for profiling float oxygen data. Journal of Geophysical Research-Oceans 2013; 118(10): 5640–5650
6. Martz TR, Connery JG, Johnson KS. Testing the Honeywell Durafet (R) for seawater pH applications. Limnology and Oceanography-Methods 2010; 8: p. 172–184
7. Johnson KS, Coletti LJ. In situ ultraviolet spectrophotometry for high resolution and long term monitoring of nitrate, bromide and bisulfide in the ocean. Deep-Sea Res. I 2002; 49: 1291–1305
8. Johnson KS, Riser SC, Karl DM. Nitrate supply from deep to near-surface waters of the North Pacific subtropical gyre. Nature 2010; 465(7301): p. 1062–1065 doi: 10.1038/nature09170 PMID: 20577212
9. Johnson KS, Coletti LJ, Jannasch HW, Sakamoto CM, Swift D, Riser SC. Long-term nitrate measurements in the ocean using the In Situ Ultraviolet Spectrophotometer: sensor integration into the Apex profiling float. Journal of Atmospheric and Oceanic Technology 2013; 30: 1854–1866.
10. Le Bris N, Sarradin P-M, Birot D, Alayse-Danet A-M. A new chemical analyzer for in situ measurement of nitrate and total sulfide over hydrothermal vent biological communities. Mar. Chem. 2000; 72: 1–15
11. Johnson KS, Needoba JA, Riser SC, Showers WJ. Chemical sensor networks for the aquatic environment. Chemical Reviews 2007; 107: 623–640 PMID: 17249737
12. Moore TS, Mullaugh K, Holyoke RR, Madison A, Yücel M, Luther GW. Marine Chemical Technology and Sensors for Marine Waters: Potentials and Limits. Annu. Rev. Mar. Sci. 2009; 1: 91–115

13. Pejcic B, Crooke E, Myers M, Ross A, Pender L, Wild-Allen K. Sensors for the detection of nutrients in aquatic environments. CSIRO Internal Report to: Flagship Collaboration Research Fund Cluster: Sensor systems for Analysis of Aquatic Environments [Project 5]. CSIRO Petroleum Resources, Perth (Report No: 09–010), 2009.
14. Wild-Allen K, Rayner M. Continuous nutrient observations capture fine-scale estuarine variability simulated by a 3D biogeochemical model. Marine Chemistry 2014; 167: 135–149.
15. Fernandez C, Farias L, Ulloa O. Nitrogen fixation in denitrified marine waters. Plos One 2011; 6(6): e20539. doi: 10.1371/journal.pone.0020539 PMID: 21687726
16. Bohlen L, Dale AW, Sommer S, Mosch T, Hensen C, Noffke A, et al. Benthic nitrogen cycling traversing the Peruvian oxygen minimum zone. Geochim. Cosmochim. Acta 2011; 75: 6094–6111
17. Dale AW, Sommer S, Ryabenko E, Noffke A, Bohlen L, Wallmann K, et al. Benthic nitrogen fluxes and fractionation of nitrate in the Mauritanian oxygen minimum zone (Eastern Tropical North Atlantic). Geochim. Cosmochim. Acta 2014; 134: 234–256
18. Jorgensen BB, Nelson DC. Sulfide Oxidation in marine sediments: Geochemistry meets microbiology. In Amend JP, Edwards KJ, Lyons TW, editors, Sufur Biogeochemistry—Past and Present. Geological Society of America Special Paper 2004; 279: 63–81.
19. Schafstall J, Dengler M, Brandt P, Bange H. Tidal induced mixing and diapycnal nutrient fluxes in the Mauritanian upwelling region. J. Geophys. Res. 2010; 115: C10014
20. Jang A, Zou Z, Lee KK, Ahn CH, Bishop PL. State-of-the art lab chip sensors for environmental water monitoring. Meas. Sci. Technol. 2011; 22: 032001 (18pp)
21. Campos CDM, da Silva JAF. Applications of autonomous microfluidic systems in environmental monitoring. RSC Advances 2003; 3: 18216–18227.
22. Sackmann EK, Fulton AL, Beebe DJ. The present and future role of microfluidics in biomedical research. Nature 2014; 507: 181–189 doi: 10.1038/nature13118 PMID: 24622198
23. Beaton AD, Cardwell CL, Thomas RS, Sieben VJ, Legiret F-E. Waugh EM, et al. Lab-on-chip measurement of nitrate and nitrite for in situ analysis of natural waters. Environ. Sci. Technol. 2012; 46: 9548–9556. doi: 10.1021/es300419u PMID: 22835223
24. Cleary J, Maher D, Diamond D (2013). Development and deployment of a microfluidic platform for water quality monitoring. In Smart Sensors for Real-Time Water Quality Monitoring, Mukhopadhyay SC and Mason A (eds.), SSMI 4 125–148. Springer Verlag Berlin
25. Provin C, Fukuba T, Okamura K, Fujii T. An integrated microfluidic system for manganese anomaly detection based on chemiluminescence: Description and practical use to discover hydrothermal plumes near the Okinawa Trough. IEEE Journal of Oceanic Engineering 2013; 38: 178–185.
26. Beaton AD, Sieben VJ, Floquet CFA, Waugh EM, Abi Kaed Bey S, Ogilvie IRG, et al. An automated microfluidic colourimetric sensor applied in situ to determine nitrite concentration. Sens. Actuators B 2011; 156: 1009–1014.
27. Horstkotte B, Duarte CM, Cerda V. Chip-on-valve concept: an integrated platform for multisyringe flow injection analysis: application to nitrite and nitrate determination in seawater. A Analytical Letters 2013; 46: 2345–2358
28. Legiret F-E, Sieben VJ, Woodward EMS, Abi Kaed Bey SK, Mowlem MC, Connelly DP, Achterberg EP. A high performance microfluidic analyzer for phosphate measurements in marine waters using the vanadomolybdate method. Talanta 2013; 116: 382–387. doi: 10.1016/j.talanta.2013.05.004 PMID: 24148419
29. Milani A, Statham PJ, Mowlem MC, Connelly DP. Development and application of a microfluidic in-situ analyzer for dissolved Fe and Mn in natural waters. Talanta 2015; 136: 15–22 doi: 10.1016/j.talanta.2014.12.045 PMID: 25702979
30. Mittelstaedt E. The ocean boundary along the northwest African coast: Circulation and oceanographic properties at the sea surface. Prog. Oceanog. 1991; 26: 307–355.
31. Stramma L, Visbeck M, Brandt P, Tanhua T, Wallace D. Deoxygenation in the oxygen minimum zone of the eastern tropical North Atlantic. Geophys. Res. Lett. 2009; 36: L20607.
32. Brandt P, Bange HW, Baynte D, Dengler M, Didwischus S-H, Fischer, et al. On the role of circulation and mixing in the ventilation of oxygen minimum zones with a focus on the eastern tropical North Atlantic. Biogeosciences 2015; 12: 489–512.
33. Mittelstaedt E. The upwelling area off Northwest Africa—a description of phenomena related to coastal upwelling, Prog. Oceanogr. 1983; 12: 307–331
34. Barton ED. The poleward undercurrent on the eastern boundary of the subtropical North Atlantic, in: Poleward flows along Eastern Ocean Boundaries, Lecture Note Series ed., edited by: Neshyba S. J., Smith R. L., and Mooers C. N. K., Springer-Verlag, 82–95, 1989

35. Sommer S, Linke P, Pfannkuche O, Schleicher T, von Deimling JS, Reitz A, et al. Seabed methane emissions and the habitat of frenulate tubeworms on the Captain Arutyunov mud volcano (Gulf of Cadiz). Mar. Ecol. Prog. Ser. 2009; 382: 69–86

36. Pfannkuche O, and the Science Party. (2014) Climate-Biogeochemistry interactions in the tropical ocean of the NW-African oxygen minimum zone (SFB754)—Cruise No. MSM17/4—March 10—April 11, 2011—Dakar (Senegal)—Las Palmas (Spain), MARIA S. MERIAN-Berichte, MSM17/4; 59 pp., DFG-Senatskommission für Ozeanographie, 10.2312/cr_msm17_4.

37. Ogilvie IRG, Sieben VJ, Floquet CF, Zmijan R, Mowlem MC, Morgan H. Reduction of surface roughness for optical quality microfluidic devices in PMMA and COC. J. Micromech. Microeng. 2010; 20: 065016.

38. Floquet CFA, Sieben VJ, Milani A, Joly EP, Ogilvie IRG, Morgan H, et al. Nanomolar detection with high sensitivity microfluidic absorption cells manufactured in tinted PMMA for chemical analysis. Talanta 2010; 84: 235–239 doi: 10.1016/j.talanta.2010.12.026 PMID: 21315925

39. Patey M, Rijkenberg M, Statham P, Stinchcombe M, Achterberg E, Mowlem MC. Determination of nitrate and phosphate in seawater at nanomolar concentrations. TrAC, Trends Anal. Chem. 2008; 27: 169–182

40. Sieben VJ, Floquet CFA, Ogilvie IRG, Mowlem MC, Morgan H. Microfluidic colourimetric chemical analysis system: Application to nitrite detection. Anal. Methods 2010; 2: 484.

41. R Core Team (2013). R: A language and environment for statistical computing. R Foundation for Statistical Computing, Vienna, Austria. Available: http://www.R-project.org/

42. Ogilvie IRG, Sieben VJ, Mowlem MC, Morgan H. Temporal Optimization of Microfluidic Colorimetric Sensors by Use of Multiplexed Stop-Flow Architecture, Anal. Chem. 2011; 82: 4814–4821.

43. Holloway PE. A comparison of semidiurnal internal tides from different bathymetric locations on the Australian north-west shelf, J. Phys. Oceanogr. 1985; 15(3): 240–251.

44. Jackson C. Internal wave detection using the Moderate Resolution Imaging Spectoradiometer 29 (MODIS), J. Geophys. Res. 2007; 112: C11012.

45. Available: http://www.robex-allianz.de/en/

46. Spencer JR, Nimmo F. Enceladus: An active icy world in the Saturn system. Annu. Rev. Earth Planet. Sci. 2013; 41: 693–717

47. Waite JH Jr, Lewis WS, Magee BA, Lunine JI, McKinnon WB, Glein CR, et al. Liquid water on Enceladus from observations of ammonia and 40Ar in the plume. Nature 2009; 460: 487–490